JOURNAL OF THE KOREAN ASTRONOMICAL SOCIETY
35: 159 ~ 174, 2002

ACCELERATION OF COSMIC RAYS AT LARGE SCALE COSMIC SHOCKS IN THE UNIVERSE

HYESUNG KANG[1] AND T. W. JONES[2]
[1]Department of Earth Sciences, Pusan National University, Pusan 609-735, Korea
[2]Department of Astronomy, University of Minnesota, Minneapolis, MN 55455, USA
E-mail: kang@uju.es.pusan.ac.kr, and twj@msi.umn.edu
(Received Oct. 18, 2002; Accepted Oct. 25, 2002)

ABSTRACT

Cosmological hydrodynamic simulations of large scale structure in the universe have shown that accretion shocks and merger shocks form due to flow motions associated with the gravitational collapse of nonlinear structures. Estimated speed and curvature radius of these shocks could be as large as a few 1000 km/s and several Mpc, respectively. According to the diffusive shock acceleration theory, populations of cosmic-ray particles can be injected and accelerated to very high energy by astrophysical shocks in tenuous plasmas. In order to explore the cosmic ray acceleration at the cosmic shocks, we have performed nonlinear numerical simulations of cosmic ray (CR) modified shocks with the newly developed CRASH (Cosmic Ray Amr SHock) numerical code. We adopted the Bohm diffusion model for CRs, based on the hypothesis that strong Alfvén waves are self-generated by streaming CRs. The shock formation simulation includes a plasma-physics-based "injection" model that transfers a small proportion of the thermal proton flux through the shock into low energy CRs for acceleration there. We found that, for strong accretion shocks, CRs can absorb most of shock kinetic energy and the accretion shock speed is reduced up to 20 %, compared to pure gas dynamic shocks. For merger shocks with small Mach numbers, however, the energy transfer to CRs is only about 10-20 % with an associated CR particle fraction of 10^{-3}. Nonlinear feedback due to the CR pressure is insignificant in the latter shocks. Although detailed results depend on models for the particle diffusion and injection, these calculations show that cosmic shocks in large scale structure could provide acceleration sites of extragalactic cosmic rays of the highest energy.

Key words : acceleration of particles – cosmology – cosmic rays – hydrodynamics – methods:numerical

I. INTRODUCTION

Shocks are ubiquitous in astrophysical environments: a few examples are Earth's bow shock, interplanetary shocks, stellar wind terminal shocks, supernova remnants, shocks in radio jets, merger shocks in intracluster media, and accretion shocks associated with large scale structure formation. Most astrophysical shocks are so-called "collisionless shocks" which form in a tenuous plasma via electromagnetic "viscosities," *i.e.,* collective electromagnetic interactions between the particles and the fields. Hence the magnetic field, especially its irregular component, is vital to the shock formation process. Our discussion will focus on a quasi-parallel shock, in which the direction of propagation is almost parallel to the magnetic field lines. According to plasma simulations of quasi-parallel shocks (Quest 1988), the particle velocity distribution has some residual anisotropy in the local fluid frame due to the incomplete isotropization during the collisionless shock formation process and so some particles can stream back upstream of the shock. Streaming motions of high energy particles against the background fluid generate strong MHD Alfvén waves upstream of the shock, which in turn scatter particles and prevent them from escaping upstream (e.g., Wentzel 1974; Bell 1978;Quest 1988;Lucek & Bell 2000). Due to these self-generated MHD waves thermal particles are confined and advected downstream, while some suprathermal particles in the high energy tail of the Maxwellian velocity distribution may re-cross the shock upstream. Then these particles are scattered back downstream by those same waves and can be accelerated further to higher energies via Fermi first order process. Hence the non-thermal, cosmic-ray particles are natural byproducts of the collisionless shock formation process and they are extracted from the shock-heated thermal particle distribution (Malkov & Völk 1998, Malkov & Drury 2001). This "thermal leakage" injection process has been observed well in the Earth's bow shock and interplanetary shocks (Ellison, Möbius, & Paschmann 1990, Baring *et al.* 1997). Also there have been observational evidence and theoretical studies that strongly support the idea that the cosmic rays are accelerated via the "diffusive shock acceleration (DSA)" process at various astrophysical shocks (*e.g.,* Drury 1983; Blandford & Eichler 1987).

According to hydrodynamic simulations of large

Corresponding Author: H. Kang

scale structure formation (*e.g.,* Kang *et al.* 1994a; Miniati *et al.* 2000), accretion shocks are formed in the baryonic component around non-linear structures collapsed from the primordial density inhomogeneities as a result of gravitational instability. Those structures can be identified as pancake-like supergalactic planes, still denser filaments, and clusters of galaxies that form at intersections of pancakes in any variants of the many cosmological models. These structures are surrounded by the hot gas heated by the accretion shocks and the CRs (ions and electrons) can be accelerated to very high energies at these shocks via the first order Fermi DSA process (Kang, Ryu & Jones 1996, Miniati *et al.* 2001a, b). The accretion shocks around the clusters of galaxies could involve flows as fast as a few 1000 kms^{-1} and, so, could be fast acceleration sites for the high energy cosmic rays up to several $\times 10^{19}$ eV, provided that the magnetic field around the clusters is order of microgauss. Norman, Melrose & Achterberg (1995) also suggested that cosmic accretion and merger shocks can be good acceleration sites for ultrahight energy CRs above $10^{18.5}$ eV if a primordial field of order $\gtrsim 10^{-9}G$ exists, or if microgauss fields can be self-generated in shocks. In fact a magnetic field with a typical strength of a few microgauss and a principal length scale of 10-100 kpc was detected in several clusters of galaxies by the Faraday rotation of radiation from distant radio sources (*e.g.,* Kim, Kronberg, Tribble 1991, Kronberg 1994, Taylor *et al.* 1994, Feretti *et al.* 1995, Clarke *et al.* 2001, Carilli & Taylor 2002). On the other hand, the magnetic fields derived from observed hard X-ray and EUV emissions, on the assumption that these are inverse Compton (IC) scattering of CMB photons, are somewhat lower ($\sim$ 0.4 microgauss) (Fusco-Femiano *et al.* 1999, 2000). The origin and evolution of cosmic magnetic fields is beyond the scope of this paper. Magnetic fields may have been injected into the ICM by radio galaxies. They may have been seeded at shocks in the course of structure formation, and then stretched and amplified up to 0.1-1 microgauss levels by turbulent flow motions in ICM and also in filaments and sheets (Kulsrud *et al.* 1997, Ryu, Kang & Biermann 1998).

Recent observations in EUV and hard X-ray have revealed that some clusters possess excess radiation compared to what is expected from the hot, thermal X-ray emitting ICM (*e.g.,* Sarazin & Lieu 1998; Lieu *et al.* 1999; Ensslin *et al.* 1999; Fusco-Femiano *et al.* 1999; Sarazin 1999). One mechanism proposed for the origin of this component is the IC scattering of cosmic microwave background photons by CR electrons accelerated by merger shocks and accretion shocks around the clusters. Also it has been suggested that the diffuse gamma-ray background radiation could originate from the same process (Loeb & Waxman 2000, Miniati 2002, Scharf & Mukherjee 2002). The same mechanisms that are capable of producing CR electrons may have produced CR protons, although the existence of CR protons in the ICM has not yet been directly observed. The existing evidence for substantial CR populations in these environments argues that nonthermal activities in the ICM could be important in understanding the dynamical status and the evolution of clusters of galaxies (Sarazin & Lieu 1998; Lieu *et al.* 1999). CR protons and electrons may provide a significant pressure to the ICM, perhaps, comparable to the thermal gas pressure (Lieu *et al.* 1999, Colafrancesco 1999), as it is for the galactic CRs in the ISM of our galaxy. Collisions of CR protons in the ICM generate a flux of γ-ray photons through the production and subsequent decay of neutral pions. While such γ-rays have not yet been detected from clusters recent estimates have shown that γ-ray fluxes from the nearest rich clusters, such as Coma, are within the range of what may be detected by the next generation of γ-ray observatories (Ensslin *et al.* 1997, Sreekumar *et al.* 1996, Miniati *et al.* 2001).

According to DSA theory a significant fraction (up to 90%) of the kinetic energy of the bulk flow associated with the strong shock can be converted into CR protons, depending the CR injection rate (Drury 1983, Jones & Kang 1990, Berezhko, Ksenofontov, & Yelshi 1995). If as much as $10^{-4} - 10^{-3}$ of the particle flux passing through the shock were injected into the CR population, the CR pressure would dominate and the nonlinear feedback to the underlying flow would become substantial. Recently Gieseler, Jones & Kang (2000) have developed a novel numerical scheme that self-consistently incorporates the thermal leakage injection based on the analytic, nonlinear calculations of Malkov (1998). This injection scheme, which has only one tightly restricted adjustable parameters, has been implemented into the combined gas dynamics and the CR diffusion-convection code with the Adaptive Mesh Refinement technique by Kang, Jones & Gieseler (2002). The CR injection and acceleration efficiencies at quasi-parallel, plane-parallel shocks were calculated with their new numerical code named as CRASH (Comic-Ray Amr SHock) code.* They found that about 10^{-3} of incoming thermal particles are injected into the CRs, that up to 60 % of initial shock kinetic energy is transferred to CRs for strong shocks, and that the shock speed is reduced up to $\sim$ 17 % for shocks with Mach number greater 30. These results have confirmed the findings of previous studies which adopted a simpler injection model that included a fully adjustable free parameter (*e.g.,* Berezhko *et al.* 1995, Kang & Jones 1995).

In this contribution we will present the numerical simulation results for quasi-parallel shocks in 1D plane-parallel geometry with the physical parameters rele-

*After this paper was accepted for publication we learned of another, recently published code dubbed "CRASH" by its authors, "Cosmological RAdiative transfer Scheme for Hydrodynamics" (Ciardi, Bianchi & Ferrara, astro-ph/0111532). There is no connection between their code and ours.

vant for the cosmological shocks emerging in large scale structure formation of the Universe. In the next section the details of numerical simulations, including the basic equations, numerical method, and model parameters, will be given. The simulation results are presented and discussed in §III, followed by a brief summary in §IV.

II. Numerical Methods

(a) Basic Equations

We solve the standard gasdynamic equations with CR pressure terms added in the conservative, Eulerian formulation for one dimensional plane-parallel geometry:

$$\frac{\partial \rho}{\partial t} + \frac{\partial (u\rho)}{\partial x} = 0, \tag{1}$$

$$\frac{\partial (\rho u)}{\partial t} + \frac{\partial (\rho u^2 + P_g + P_c)}{\partial x} = 0, \tag{2}$$

$$\frac{\partial (\rho e_g)}{\partial t} + \frac{\partial (\rho e_g u + P_g u + P_c u)}{\partial x} = -L(x,t), \tag{3}$$

$$\frac{\partial S}{\partial t} + \frac{\partial (uS)}{\partial x} = 0, \tag{4}$$

where $P_{\rm g}$ and $P_{\rm c}$ are the gas and the CR pressure, respectively, $e_{\rm g} = P_{\rm g}/[\rho(\gamma_{\rm g} - 1)] + u^2/2$ is the total energy density of the gas per unit mass and the rest of the variables have their usual meanings. The injection energy loss term, $L(x,t)$, accounts for the energy of the suprathermal particles injected to the CR component at the subshock. Here, $S = P_g/\rho^{\gamma_g - 1}$, the "Modified Entropy", is introduced in order to follow the preshock adiabatic compression accurately in strong CR modified shocks. We note that the equation (4) is valid only outside the dissipative subshock; *i.e.*, where the gas entropy is conserved. Hence the modified entropy equation is solved outside the subshock, while the total energy equation is applied across the subshock.

The diffusion-convection equation for the pitch angle averaged CR distribution function, $f(p,x,t)$, *e.g.*, Skilling 1975) is given by

$$\frac{\partial f}{\partial t} + u\frac{\partial f}{\partial x} = \frac{1}{3}\left(\frac{\partial u}{\partial x}\right) p\frac{\partial f}{\partial p} + \frac{\partial}{\partial x}\left(\kappa(x,p)\frac{\partial f}{\partial x}\right). \tag{5}$$

and $\kappa(x,p)$ is the spatial diffusion coefficient. For convenience we always express the particle momentum, p in units $m_{\rm p}c$. As in our previous studies, the function $g(p) = p^4 f(p)$ is evolved instead of $f(p)$ and $y = \ln(p)$ is used instead of the momentum variable, p for that step. Then the CR pressure is calculated from the nonthermal particle distribution as follows:

$$P_{\rm c} = \frac{4}{3}\pi m_{\rm p} c^2 \int_0^\infty g(p)\frac{{\rm d}p}{\sqrt{p^2+1}}. \tag{6}$$

(b) CRASH: CR/AMR Hydrodynamics Code

Unlike ordinary gas shocks, the CR shock includes a wide range of length scales associated not only with the dissipation into "thermal plasma", but also with the nonthermal particle diffusion process. Those are characterized by the so-called diffusion lengths,

$$D_{\rm diff}(p) = \kappa(p)/u, \tag{7}$$

where $\kappa(p)$ is the spatial diffusion coefficient for CRs of momentum p, and u is the characteristic flow velocity (Kang & Jones 1991). Accurate solutions to the CR diffusion-convection equation require a computational grid spacing significantly smaller than $D_{\rm diff}$, typically, $\Delta x \sim 0.1 D_{\rm diff}(p)$. On the other hand, for a realistic diffusion transport model with a steeply momentum-dependent diffusion coefficient, the highest energy, relativistic particles have diffusion lengths many orders of magnitude greater than those of the lowest energy particles.

To follow the acceleration of highly relativistic CRs from suprathermal energies, all those scales need to be resolved numerically. However, the diffusion and acceleration of the low energy particles are important only close to the shock owing to their small diffusion lengths. Thus it is necessary to resolve numerically the diffusion length of the particles only around the shock. To solve this problem generally we have developed the CRASH code by combining a powerful "Adaptive Mesh Refinement" (AMR) technique (Berger & Le Veque 1998) and a "shock tracking" technique (Le Veque & Shyue 1995), and implemented them into a hydro/CR code based on the wave-propagation method (Kang *et al.* 2001; Kang *et al.* 2002). The AMR technique allows us to "zoom in" inside the precursor structure with a hierarchy of small, refined grid levels applied around the shock. The shock tracking technique follows hydrodynamical shocks within regular zones and maintains them as true discontinuities, thus allowing us to refine the region around the gas subshock at an arbitrarily fine level. The result is an enormous savings in both computational time and data storage over what would be required to solve the problem using more traditional methods on a single fine grid.

(c) Injection Model

In the "thermal leakage" injection model, some suprathermal particles in the tail of the Maxwellian distribution swim successfully against the Alfvén waves advecting downstream, and then leak upstream across the subshock and get injected in the CR population. In order to model this injection process in Gieseler *et al.* (2001) we adopted a "transparency function", $\tau_{\rm esc}$, which expresses the probability that supra-thermal particles at a given velocity can leak upstream through the magnetic waves, based on non-linear particle interactions with self- generated waves (Malkov and Völk 1998). In this scheme, the transparency function is *ap-*

proximated by the following functional form,

$$\tau_{\rm esc}(\epsilon, v/u_d) = H[\tilde{v} - (1+\epsilon)] \left(1 - \frac{u_d}{v}\right)^{-1} \left(1 - \frac{1}{\tilde{v}}\right) \cdot \exp\left\{-[\tilde{v} - (1+\epsilon)]^{-2}\right\}, \quad (8)$$

which depends on the ratio of particle velocity, v, to downstream flow velocity in the subshock rest-frame, u_d. Here H is the Heaviside step function. The inverse wave-amplitude parameter, $\epsilon = B_0/B_\perp$, is defined in Malkov and Völk (1998) and measures the ratio of the amplitude of the postshock MHD wave turbulence $B_\perp$ to the general magnetic field aligned with the shock normal, B_0. Here $\tilde{v} = \epsilon\, v/u_d$ is the normalized particle velocity. This function behaves like a smoothed step function, and the injection takes place in momentum space where the $\partial\tau_{\rm esc}/\partial p$ is greatest. The breadth of the thermal velocity distribution relative the downstream flow velocity in the subshock rest-frame (*i.e.*, $v_{\rm th}/u_d$) determines the probability of leakage, and so the injection process is sensitive to the velocity jump at the subshock, which depends on the subshock Mach number. The injection rate increases with the subshock Mach number, but becomes independent of M_s in the strong shock limit of $M_s \gtrsim 10$ (Kang *et al.* 2002). Thus the injection rate should change with the shock strength in the time-dependent evolution of CR modified shocks, as the subshock weakens by way of precursor compression.

The only free parameter of the adopted transparency function is ϵ and it is rather well constrained, since $0.3 \lesssim \epsilon \lesssim 0.4$ is indicated for strong shocks (Malkov & Völk 1998). However, it turns out the injection rate depends sensitively on the value of ϵ, due to the exponential cut off in a thermal velocity distribution. It is also expected that the wave generation is weaker for low Mach shocks, leading to the larger values of ϵ. So in this study we will consider $0.2 \le \epsilon \le 0.4$.

In the CRASH code, in order to emulate numerically thermal leakage injection, we first estimate the number of suprathermal particles that cross the shock according to the diffusion-convection equation, and then we allow only a small fraction of the combined advective and diffusive fluxes to leak upstream with the probability prescribed by $\tau_{\rm esc}$. The readers are referred to Kang *et al.* (2002) for more details of our numerical scheme for thermal leakage injection model.

III. Numerical Model

(a) Diffusion Coefficient Model

Diffusive acceleration at shocks depends on the existence of Alfvénic turbulence capable of strongly scattering energetic protons. The irregularities in the magnetic field within the cluster can be generated by various dynamical effects such as the supersonic motion of galaxies through ICM, mergers of substructures and galactic winds. In addition, according to the cosmological hydrodynamic simulations, the downstream regions of the accretion shocks (*i.e.*, ICM) are full of turbulent flow motions. Some observations (Feretti *et al.* 1995) indicate that the ICM field is likely to be tangled on scales of the order of less than 1 kpc. Then turbulent flows may subsequently generate the irregularities in magnetic field. Outside the accretion shock, however, we must hypothesize the existence of pre-existing field turbulence. Lucek & Bell (2000) have shown by numerical simulations that CR streaming induces large-amplitude Alfvén waves in a quasi-parallel shock, implying that the shock formation process itself can generate the necessary turbulent field. So it is commonly assumed in calculations of diffusive shock acceleration that the scattering Alfvén waves are self-generated by the CRs themselves by the so-called "streaming instability" (Wentzel 1974). Adiabatic compression of that field and turbulence by convergence of the inflow onto the accretion shock might very reasonably lead to an acceptable level of magnetic irregularities in the shock vicinity.

The Bohm diffusion model represents a saturated wave spectrum and gives the minimum diffusion coefficient as $\kappa_{\rm B} = 1/3 r_{\rm g} v$, when the particles scatter within one gyration radius ($r_{\rm g}$) due to random scatterings off the self-generated waves. This gives

$$\kappa(p) = \kappa_{\rm o} \frac{p^2}{(p^2+1)^{1/2}}, \quad (9)$$

where $\kappa_{\rm o} = 3.13 \times 10^{22} {\rm cm^2 s^{-1}} B_\mu^{-1}$ and B_μ is the magnetic field strength in units of microgauss. In order to model amplification of self-generated turbulent waves due to compression of the perpendicular component of the magnetic field, the spatial dependence of the diffusion is modeled as

$$\kappa(x,p) = \kappa(p) \left(\frac{\rho_0}{\rho(x)}\right), \quad (10)$$

where ρ_0 is the upstream gas density. This form is also required to prevent the acoustic instability of the precursor (Kang, Jones & Ryu 1992).

(b) Time and Length Scales

The mean acceleration time scale for a particle to reach momentum p is determined by the velocity jump at the shock and the diffusion coefficient (e.g., Drury 1983), that is,

$$\tau_{acc} = \frac{p}{< \frac{dp}{dt} >} = \frac{3}{u_1 - u_2} \left(\frac{\kappa_1}{u_1} + \frac{\kappa_2}{u_2}\right). \quad (11)$$

Here the subscripts, 1 and 2, designate the upstream and downstream conditions, respectively. If the strong shock limit is taken (*i.e.*, $u_2 = u_1/4$), and we assume for a turbulent field that B/ρ is constant across the shock (*i.e.*, κ/u = constant), then $\tau_{acc} \approx 8\kappa_{\rm B}/u_s^2$. Using the Bohm diffusion coefficient in equation (9), the mean

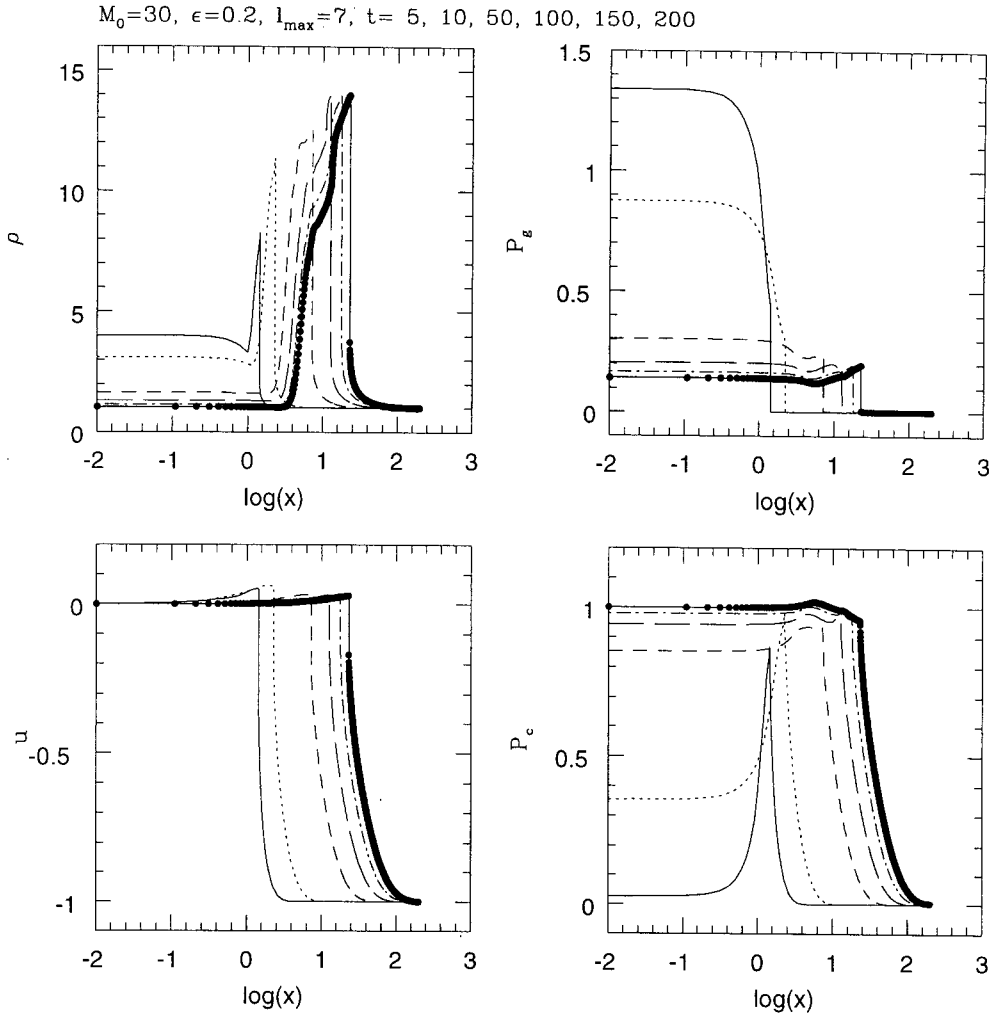

Fig. 1.— Time evolution of the shock driven by an accretion flow with $\rho_0 = 1$, $u_0 = -1$ and $M_0 = 30$ which is reflected at $x = 0$. Seven levels of refinements ($l_{\rm max} = 7$) were used and the inverse wave-amplitude parameter $\epsilon = 0.2$ was adopted. The snapshots are shown at $t = 5$, 10, 50, 150, and 200. The shock propagates to the right, so the leftmost profile corresponds to the earliest time. For $t = 200$, data at each cell is shown as filled circles to show clearly the subshock jump. Note the distance from the reflecting plane is in a logarithmic scale.

acceleration time scale is given by

$$\tau_{acc} \approx (7.92\times10^9 \text{years}) \left(\frac{p}{10^{10}}\right) B_\mu^{-1} \left(\frac{u_s}{1000\text{km s}^{-1}}\right)^{-2}. \quad (12)$$

This shows that the diffusive acceleration time scale increases directly with the particle energy and that it takes about a billion years to accelerate the proton to $E = 10^{18}$eV at a typical cluster shock, assuming $B_\mu \sim 1$. The diffusion length of the CR protons is given by

$$D_{\rm diff} = \frac{\kappa_{\rm B}}{u_s} = 1.02\text{Mpc} \left(\frac{p}{10^{10}}\right) B_\mu^{-1} \left(\frac{u_s}{1000\text{km s}^{-1}}\right)^{-1}. \quad (13)$$

So the CR protons of $E = 10^{18}$eV diffuse on the length scale comparable to the cluster size. Note the mildly relativistic protons ($p \sim 1 - 10$) are almost instantaneously accelerated at these shocks compared to the cosmological time scale and diffuse on the length scale much smaller than the cosmological scale.

(c) 1D Plane-parallel Shock Models

In this contribution, we study the CR acceleration and its dynamical effects at one-dimensional (1D) quasi-parallel shocks which form due to the accretion flows in a plane-parallel geometry. In general, cosmic shocks associated with large scale structure formation can be oblique and have various geometries, depending on the types of nonlinear structure onto which the accretion flow falls. Roughly speaking we have: 1D plane-parallel shocks around the sheets, 2D cylindrical shocks around the filaments, and 3D spherical shocks around the clusters of galaxies. Due to severe requirements on the computational resources, our simulations can follow the acceleration of the protons from suprathermal ener-

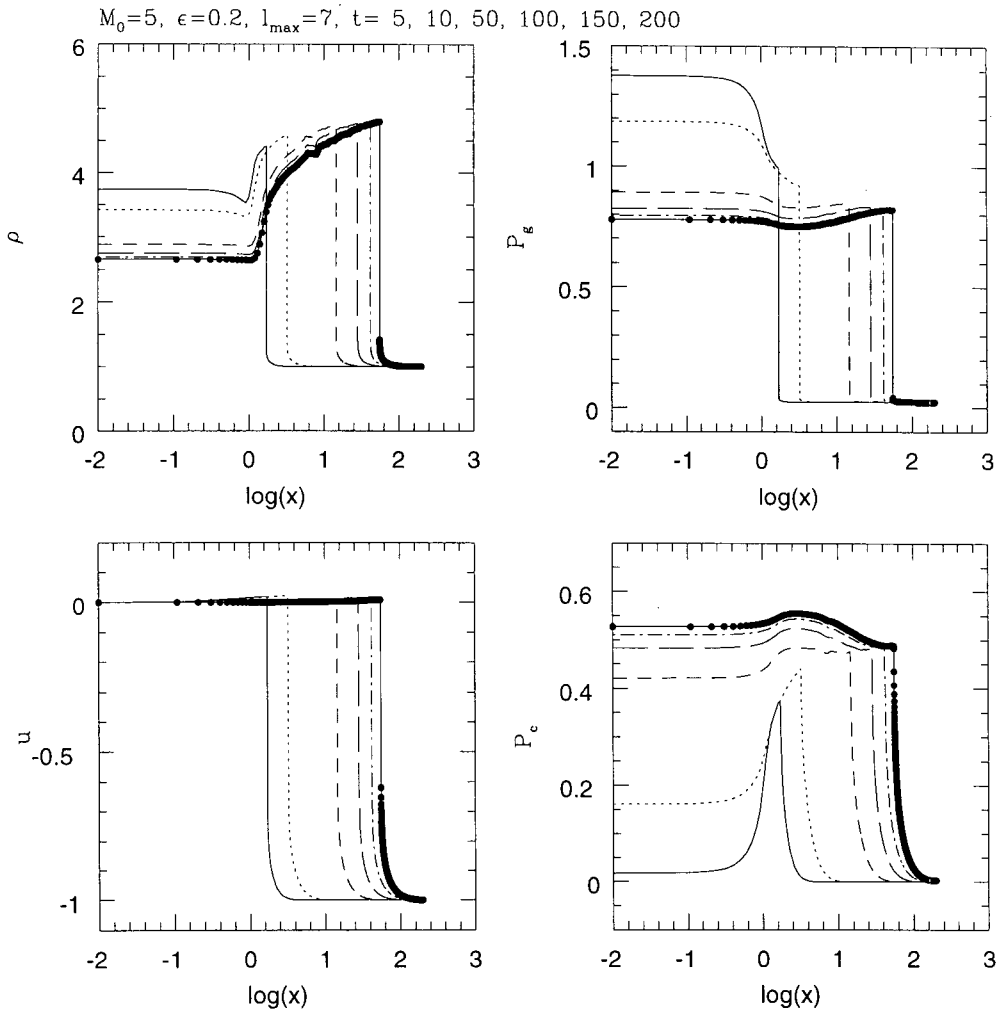

Fig. 2.— Same as Figure 1 except $M_0 = 5$.

gies ($p \sim 10^{-3}$) to mildly relativistic energies ($p \sim 50$). For the particles in this energy range, the acceleration time scales (< 40 years) are much shorter than and the cosmological time scale ($t_{\rm H} \sim 10^{10}$ years) and the diffusion length scales (< 0.1pc) are much smaller than the curvature of multi-dimensional cosmic shocks ($R_s \sim$ a few Mpc). On those scales where $D_{\rm diff} \ll R_s$, the diffusion and acceleration of CRs can be studied with the 1D plane-parallel shock models. Thus, for our purposes the shocks that occur in major mergers of substructures can be represented approximately by 1D plane-parallel shocks. As shown in Kang *et al.* (2002), the maximum CR pressure and the shock structure modification approach to time asymptotic limits as the particles become relativistic $p \sim 1$. This is due to the balance between acceleration and diffusion of CRs, that is, fewer particles are accelerated to higher energies, and higher energy CRs diffuse over larger volume of space as the CR shock evolves. Thus our simulations can predict long-term behaviors of CR modified shocks, even though our integration time is only a small fraction of t_H.

Here we ignore gravity, so changes in the infall velocity and density, and the background cosmological evolution, because the integration time of our simulations is much shorter than any of the cosmological time scales. So we consider a pancake shock formed by the steady accretion flow with a constant density and pressure: a 1D simulation box with $[0,x_{max}]$ and an accretion flow entering into the right boundary of the simulation box with a constant density, ρ_0, pressure, $P_{g,0}$, and velocity, u_0. The flow is reflected at the left boundary ($x = 0$) (*i.e.,* pancake middle plane). A shock forms and propagates to the right. For a hydrodynamic shock without the CRs, the shock speed is $u_s = |u_0|/(r-1)$ in the simulation frame and $u_s' = |u_0|r/(r-1)$ in the far upstream rest frame, where r is the compression ratio across the shock. Throughout the paper we denote the velocities in the simulation frame by the unprimed variables, while the velocities in the rest frame of far upstream flow by the primed variables. For strong hydrodynamics shocks, $r = 4$ and $u_s' = (4/3)|u_0|$. A CR

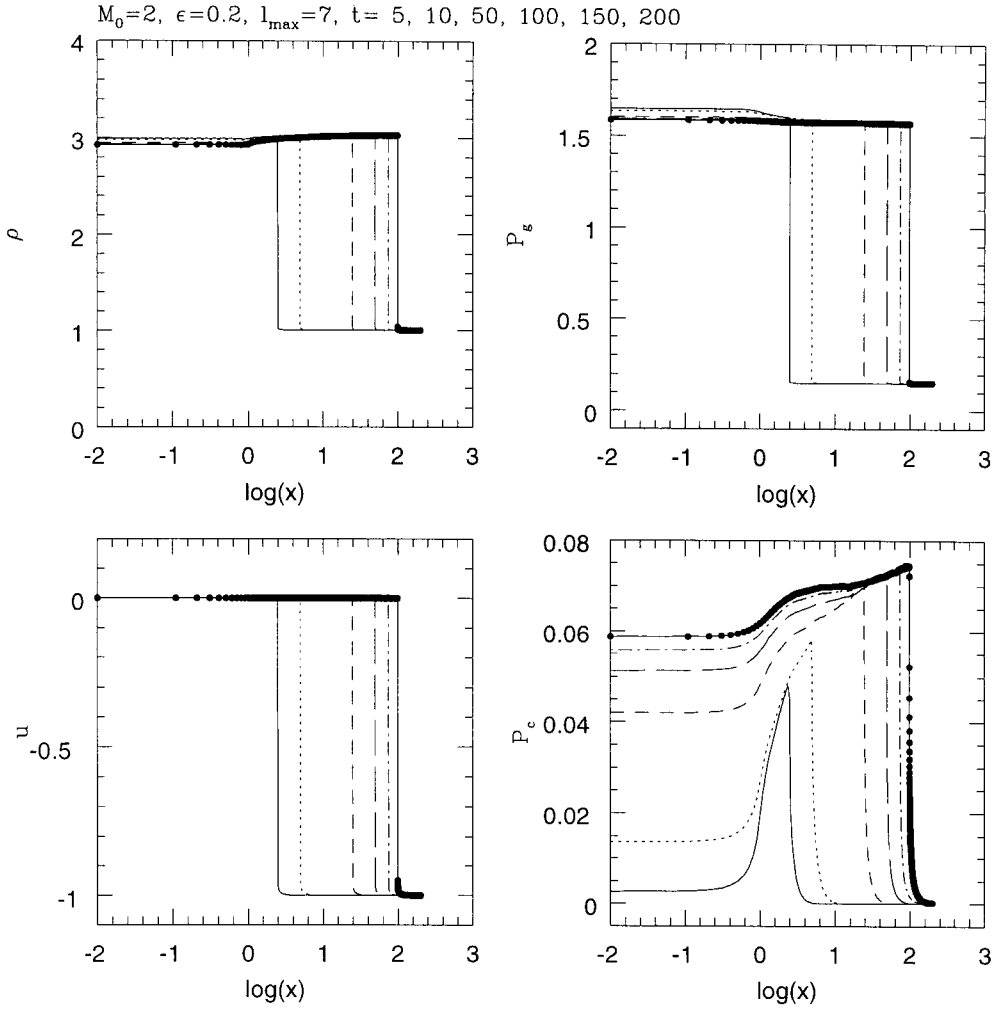

Fig. 3.— Same as Figure 1 except $M_0 = 2$.

modified shock consists of a smooth precursor and a subshock, since the CRs diffuse upstream of the subshock, and the CR pressure decelerates and heats the preshock flow adiabatically, resulting in weakening of the subshock. We denote the values immediately upstream of the subshock as u_1, ρ_1, and $P_{g,1}$ and the values immediately downstream of the subshock as u_2, ρ_2 and $P_{g,2}$. We also denote the subshock speed relative to the immediate upstream flow as u_{sub}, which is smaller than u_s' due to the precursor deceleration.

We designate the shock models by the Mach number of the accretion flow that is defined by

$$M_0 = \frac{|u_0|}{(\gamma P_{g,0}/\rho_0)^{1/2}}, \qquad (14)$$

where once again u_0, ρ_0, $P_{g,0}$ are the accretion velocity, the density and pressure of the infall flow, respectively. The Mach number of the accretion shock resulting from such accretion flow is $M_s \approx 4/3M_0$ for strong gasdynamic shocks. We set the far upstream density and flow values as $\rho_0 = 1$, $u_0 = -1$ in code units for all models, while we vary the gas pressure, $P_{g,0}$ for different values of M_0, where $2 \leq M_0 \leq 100$. So the preshock gas is colder for high values of M_0.

The following parameters are used: the gas adiabatic index, $\gamma_g = 5/3$ and the velocity normalization constant $u_o = 1500$ kms^{-1} ($\beta = u_o/c = 0.005$). Then the diffusion coefficient, $\kappa_o = 3.13 \times 10^{21}$cm^{2}s$^{-1}B_\mu^{-1}$, determines the length and time scales as $x_o = \kappa_o/u_o$ and $t_o = \kappa_o/u_o^2$, respectively, which represent, in fact, the diffusion length and time scales for the protons of $p = 1$. For $B_\mu = 1$, $x_o = 2.1 \times 10^{14}$ cm and $t_o = 1.4 \times 10^6$s. These scales are much smaller than cosmological length and time scales as discussed before, which justifies our assumptions about the steady accretion flow and the 1D plane-parallel geometry. The gas density and pressure normalization constants, ρ_o and $P_o = \rho_o u_o^2$, are arbitrary. For the hydrogen number density of $n_H = 10^{-4}$cm^{-3}, for example, $\rho_o = 2.34 \times 10^{-28}$g cm^{-3} and $P_o = 5.26 \times 10^{-12}$erg cm^{-3}. So if one assumes the Bohm diffusion model, the three parameters, *i.e.*, β, B_μ, and M_0, sufficiently define a CR shock model.

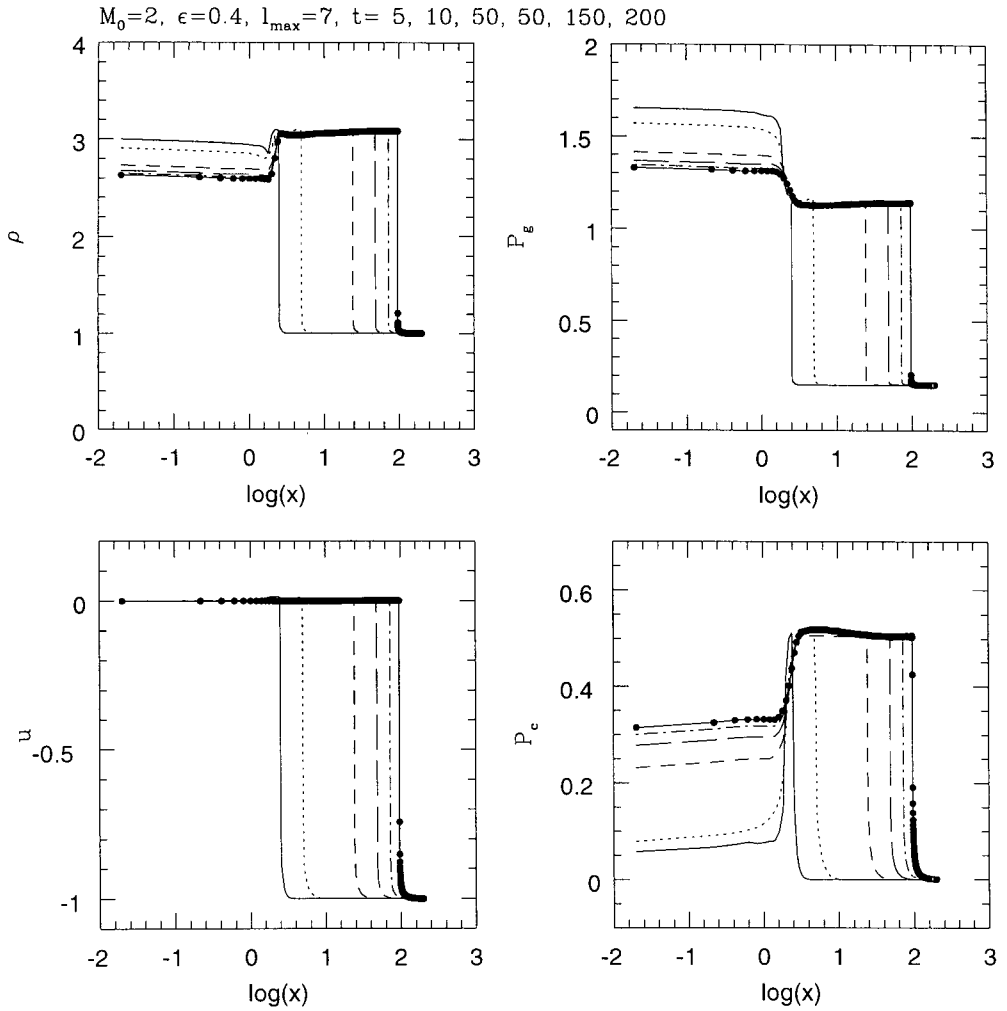

Fig. 4.— Same as Figure 1 except $M_0 = 2$ and $\epsilon = 0.4$.

Throughout the paper and in the code physical variables are given in units of the normalization constants, x_o, t_o, u_o, ρ_o, and P_o.

Although the theoretically preferred values of the inverse wave-amplitude parameter, ϵ, lie between 0.3 and 0.4 for strong shocks (Malkov 1998), such values lead to very efficient initial injection and most of the shock energy is transfered to the CR component for strong shocks of $M_0 \gtrsim 30$ (Kang *et al.* 2002). As a more conservative option we have considered a set of models for $2 \leq M_0 \leq 100$ with $\epsilon = 0.2$ and another set of models for $M_0 = 2$ with $0.2 \leq \epsilon \leq 0.4$. The former is chosen to explore the dependence of the CR acceleration on the accretion flow Mach number for a given value of ϵ, while the latter is chosen to explore the dependence on the injection rate for a low Mach number flow.

The simulations were carried out on a base grid with $\Delta x_0 = 0.02$ using $l_{\rm max} = 7$ additional grid levels, so $\Delta x_7 = 1.56 \times 10^{-4}$ on the finest grid. The simulated space is $x = [0, 200]$ and $N = 10000$ zones are used on the base grid for the models that were integrated to $t/t_o = 200$. For the models that were integrated to $t/t_o \lesssim 100$, $x = [0, 100]$ and $N = 5000$ are used. The number of refined zones around the shock is $N_{rf} = 100$ on the base grid and so there are $2N_{rf} = 200$ zones on each refined level. The length of the refined region at the base grid is 2, so 1/100 of the entire simulated space on the base grid is refined. To avoid technical difficulties, the multi-level grids are used only after the shock propagates away from the left boundary at the distance of $x_s = 1$. With $x_s < 1$, the downstream refined region is outside the left boundary of the simulation box and the full length of the refined region around the shock cannot be set down with the current version of the CRASH code. After the shock moves to $x_s = 1$ (at $t \approx 3$ for strong shocks), the AMR technique is used and the CR injection and acceleration are activated. This initial delay of the CR injection and acceleration should not affect the final outcomes. We integrate the simulation until $t = 100 - 200$, so that the maximum momentum achieved by the end of simulation is of order

of $p_{\rm max} \sim 40$, above which the CR distribution function decreases exponentially. For all models we use 230 uniformly spaced logarithmic momentum zones in the interval $\log(p/m_p c) = [\log p_0, \log p_1] = [-3.0, +3.0]$

For gasdynamic variables the continuous boundary condition is used at right boundary, while the reflecting boundary condition is applied to left boundary of the simulation box. For the CR distribution function a continuous boundary is assumed for the advection step and a no-flux boundary condition is adopted for the spatial diffusion step. Either below p_0 or above p_1; $g(p) = 0$ is assumed.

IV. RESULTS

(a) Modified Shock Structure

We show the time evolution of shocks at $t = 5$, 10, 50, 100, 150 and 200 for models with the accretion flow Mach number, $M_0 = 30$, 5, and 2 in Figures 1-3. The inverse wave amplitude parameter was assumed to be $\epsilon = 0.2$. As CRs are injected and accelerated at the shock, the CR pressure increases and diffuses upstream, leading to a precursor in which the upstream flow is decelerated and compressed adiabatically. As the CR precursor grows, the subshock slows down and the postshock density increases, while the postshock gas pressure decreases. Because the injection rate is quite high for strong shocks, the CR energy increases and the modification to the flow structure proceeds very quickly in a time scale comparable to $t_{\rm acc}$ for $p \sim 2 - 3$.

Kang *et al.* (2002) also considered similar shock models, but with different flow conditions at the left boundary. There a gasdynamic shock was set up initially and allowed to evolve with open boundaries both far upstream and downstream. Because the CRs are not allowed to diffuse out at the reflecting, downstream boundary in the current models, the CR pressure builds up faster. Otherwise, however, the CR shocks evolve similarly in both models: 1) The total transition consists of a precursor and a subshock that weakens to a lower Mach number shock, but does not disappear entirely. 2) After an initial quick adjustment, the CR pressure at the shock reaches *approximate* time-asymptotic values when the fresh injection and acceleration are balanced with advection and spreading of high energy particles due to strong diffusion. For strong shocks, $P_{\rm c,2}/\rho_0(u'_{s,0})^2 \to 0.56$, where $u'_{s,0}$ is the shock speed before any significant nonlinear CR feedback occurs. 3) Once the postshock CR pressure becomes constant, the shock structure evolves approximately in a "self-similar" way, because the scale length of shock broadening increases linearly with time. 4) A postshock "density spike" forms due to the nonlinear feedback of the CR pressure (see also Jones & Kang 1990). 5) For a given inverse wave-amplitude parameter, ϵ, the CR acceleration efficiency and the flow modification depend sensitively on the shock Mach number, but they seem to converge at the strong shock limit ($M_s \gtrsim 30$).

For the $M_0 = 30$ model, for example, the initial unmodified shock speed is $u'_{s,0} = 4/3$ (Mach number $M_s = 40$), but the shock slows down to $u'_s \approx 1.1$ due to CR nonlinear modification. So the ratio $P_{\rm c,2}/\rho_0(u'_s)^2 \to 0.8$, where u'_s is the instantaneous shock speed. For strong shocks the CR pressure dominates over the gas pressure with a CR injection fraction $\sim 10^{-4} - 10^{-3}$ (see Figure 8 below), and a ratio $P_{\rm c,2}/\rho_0(u'_s)^2 \to 0.8 - 1.0$, which is consistent with the simulation results of Kang *et al.* (2002). For the $M_0 = 5$ model, $P_{\rm c,2}/\rho_0(u'_{s,0})^2 \to 0.27$ and still shows substantial degree of the flow modification. For $M_0 = 2$ model, however, the CR pressures increases only to $P_{\rm c,2}/\rho_0(u'_s)^2 \sim 0.03$ and the flow structure is not modified at all. According to Miniati *et al.* (2000), the cosmic shocks inside the ICM (*i.e.,* merger shocks) have mostly low Mach numbers of $1 \lesssim M_s \lesssim 5$, because these shocks propagate into the already hot medium. But the shock speed is not much different from the accretion shocks that propagate into the cold medium and so have high Mach numbers. Thus the sample models shown in Figures 1-3 can provide qualitative pictures on the effects of the CR acceleration to dynamics of cosmological shocks.

We note, however, that the value of $\epsilon = 0.2$ is perhaps unrealistically small for a low Mach number shock, since the self-generation of waves is expected to be less efficient. So, we considered three additional models for $M_0 = 2$ ($M_s = 3$) with larger values of $\epsilon = 0.25$, 0.3, and 0.4. The CR pressure increases with higher values of ϵ due to higher leakage fractions, as expected. So, for example, the ratio $P_{\rm c,2}/\rho_0(u'_s)^2 \sim 0.22$ for $\epsilon = 0.4$ model (see Figure 4). But even in this rather high injection model with a CR fraction of $\xi \sim 10^{-2}$, the flow modification is minimal except for the reduction of the gas pressure. As expected, the CR acceleration is very inefficient and the CR nonlinear feedback is insignificant in weak shocks of a Mach number of a few.

(b) Particle Distribution Function

Evolution of the CR distribution function at the shock is given for the models of $M_0 = 30, 10, 5$, and 2 with $\epsilon = 0.2$ in Figure 5. Thermal particles are represented by a Maxwellian distribution below $p \sim 10^{-2}$. One can see that the Maxwellian distribution shifts to lower momenta, as the postshock temperature reduces due to energy transfer to CRs. Just above the injection pool, the distribution function changes smoothly from the thermal distribution to an approximate power-law whose index is close to the test–particle slope for the subshock. While a fraction of particles injected earlier continues to be accelerated to higher momenta, so that $p_{\rm max}(t)$ increases, the amplitude of $g(p)$ at the shock and at a given momentum decreases with time for $p < p_{\rm max}(t)$ due to diffusion. The distribution function $g(p)$ shows the characteristic "concave upwards" curves reflecting modified shock structure (including

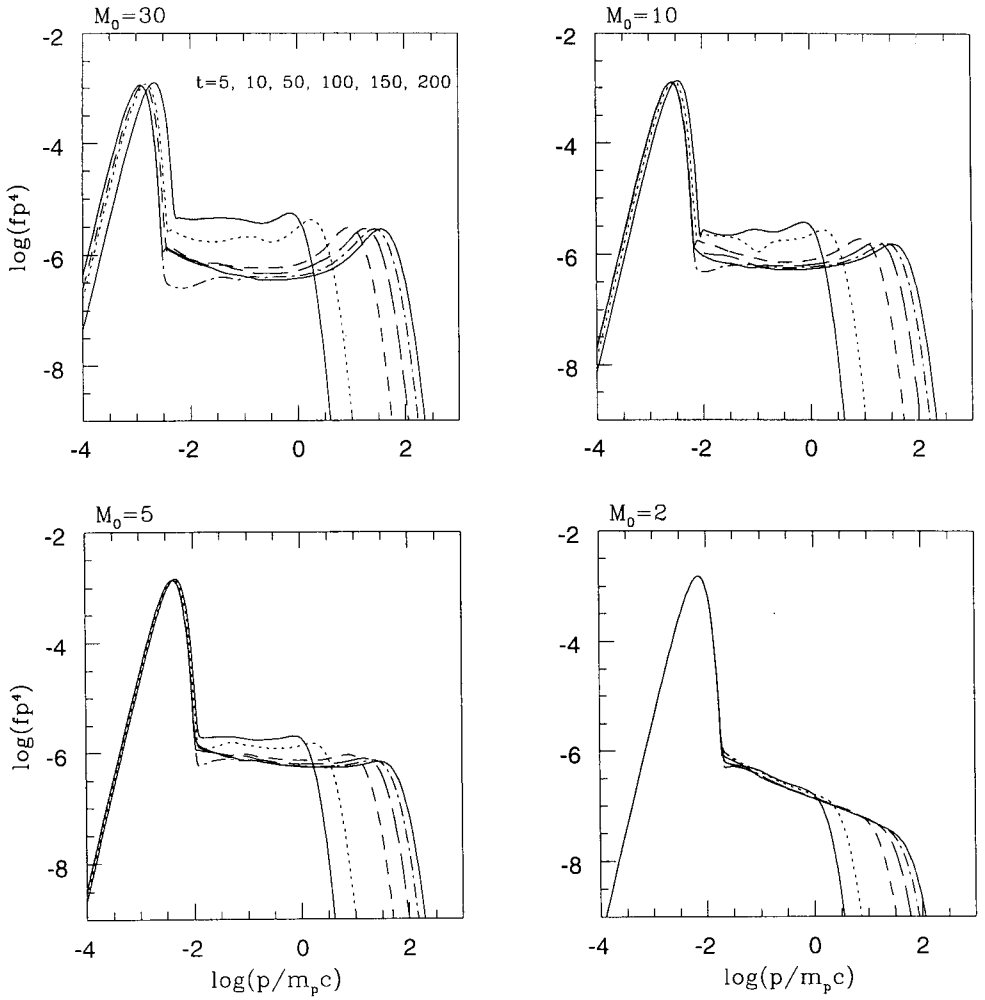

Fig. 5.— Evolution of the CR distribution function at the shock, represented as $g = p^4 f(p)$, is plotted for the models of $M_0 = 30$, 10, 5, and 2 with $\epsilon = 0.2$.

the precursor) for the shocks with $M_0 \geq 10$. For the models with $M_0 = 2$ and $\epsilon = 0.2$, the CR modification to the flow structure is insignificant, so the particle distribution is a power-law with the test-particle slope (*i.e.*, $f(p) = f_0 p^{-q}$ and $q = 3r/(r-1) \approx 4.5$, where $r = 3$ for $M_s = 3$).

In Figure 6, the CR distribution function at the shock is shown for the $M_0 = 2$ model for $\epsilon = 0.2$, 0.25, 0.3, and 0.4. For weaker wave fields (larger ϵ) the particles with lower momenta can leak upstream, so the injection pool is located at the lower momenta closer to the peak of the Maxwellian distribution, resulting in a higher injection rate. Even though about 20 % of the shock kinetic energy is transfered to the CR component for $\epsilon = 0.4$, the flow velocity structure is only slightly affected. So the CR distribution function is dictated by the test-particle like power-law spectrum for $M_0 = 2$ models, roughly independent of the value of ϵ.

(c) Subshock Evolution

The speed of the "initial hydrodynamic shock", $u'_{s,0}$, that emerges from the reflecting plane before the CR injection/acceleration begins depends on the Mach number of the accretion flow. It is given by $u'_{s,0} = r/(r-1)|u_0|$, so that $u'_{s,0} = 1.5$ for $M_0 = 2$, $u'_{s,0} = 1.36$ for $M_0 = 5$, and $u'_{s,0} = 4/3$ for $M_0 \geq 10$. After the CR injection/acceleration starts, the CR pressure modifies the shock flow and the "instantaneous shock" speed relative to the far upstream flow, u'_s, decreases. We plotted the position of the shock, x_s, against time for models with $\epsilon = 0.2$ in the upper left panel of Figure 7. We see that the shock is decelerated further in higher Mach number models, since the CR pressure is greater and so is its dynamical feedback to the flow.

The injection rate in the thermal leakage injection model depends on the strength of the subshock, so the subshock speed relative to the immediate preshock gas in the precursor, $u_{\rm sub}$, is important. Because of the

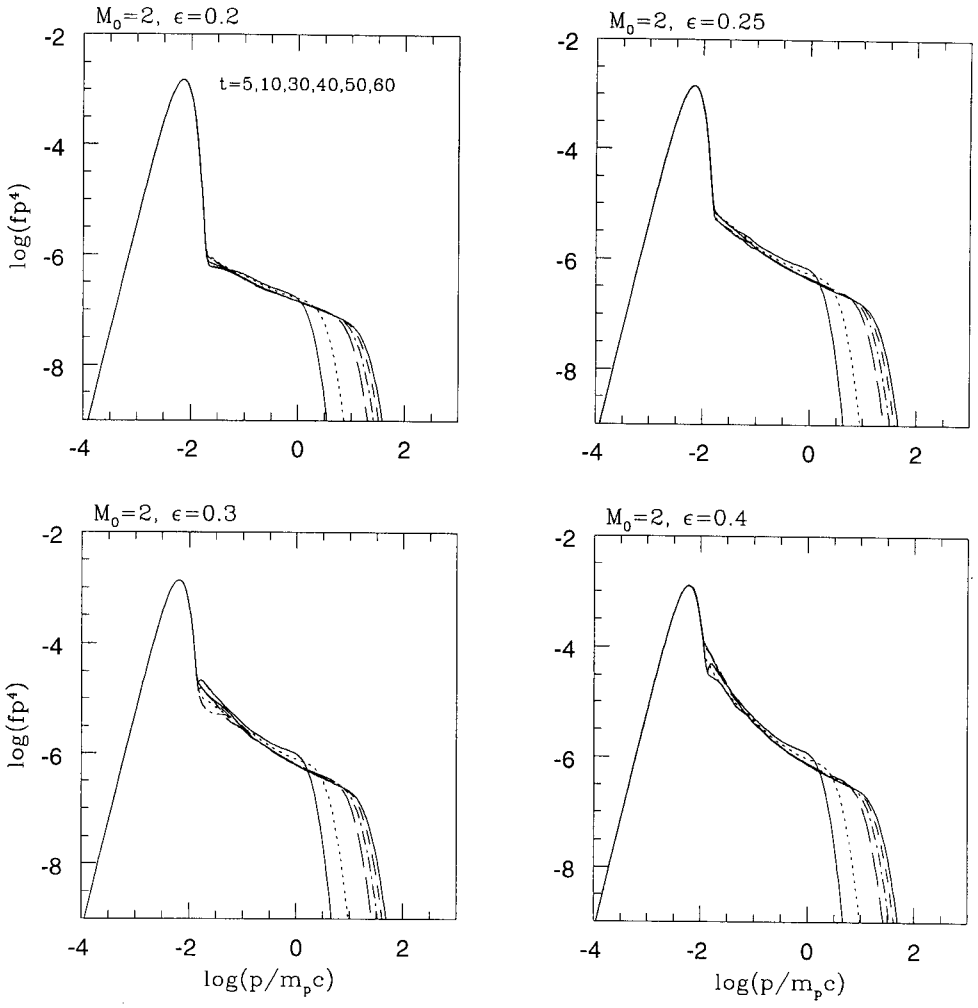

Fig. 6.— Evolution of the CR distribution function at the shock, represented as $g = p^4 f(p)$, is plotted for the $M_0 = 2$ models with $\epsilon = 0.2$, 0.25, 0.3 and 0.4.

pre-deceleration in the precursor, especially for strong shocks, $u_{\rm sub}$ can be much smaller than the shock speed relative to the far upstream. We plotted this subshock speed in the upper right panel of Figure 7. For $M_0 = 2$ $u_{\rm sub} \approx u_s'$, but $u_{\rm sub} \ll u_s'$ for $M_0 \geq 30$. We also plotted the pre-subshock gas density, ρ_1/ρ_0, and the immediate postshock gas density, ρ_2/ρ_0, in the lower two panels. The modification to the flow velocity occurs mostly before $t \lesssim 10$, so the subshock velocity decreases at the same time, but the precursor compression continues even after $t > 10$, especially in the strong shocks. We note that the subshock persists and so a completely smooth transition never develops by the termination time of our simulations.

(d) Injection and Acceleration Efficiencies

We define the injection efficiency as the fraction of particles that have entered the shock from far upstream and then injected into the CR distribution:

$$\xi(t) = \frac{\int_0^{x_{max}} {\rm dx} \int_{p_0}^{p_1} 4\pi f_{\rm CR}(p,x,t) p^2 {\rm dp}}{\int_{t_1}^{t} n_0 u_s'(t') {\rm dt}'} \qquad (15)$$

where $f_{\rm CR}$ is the CR distribution function, n_0 is the particle number density far upstream, and t_1 is the time when the CR injection/acceleration is turned on ($t_1 \approx 3$ for $M_0 \geq 5$ and $t \approx 2$ for $M_0 = 2$). If the subshock becomes steady, then $n_0 u_s'$ is the same as the particle flux swept by the subshock, $n_1 u_{\rm sub}$, where n_1 is the particle number density immediately upstream to the subshock. In our simulations these two fluxes can differ up to 10 % for strong shock models, because the shock speed is changing slowly.

As a measure of acceleration efficiency, we define the "CR energy ratio"; namely the ratio of the total CR energy within the simulation box to the kinetic energy in the *initial shock frame* that has entered the simulation

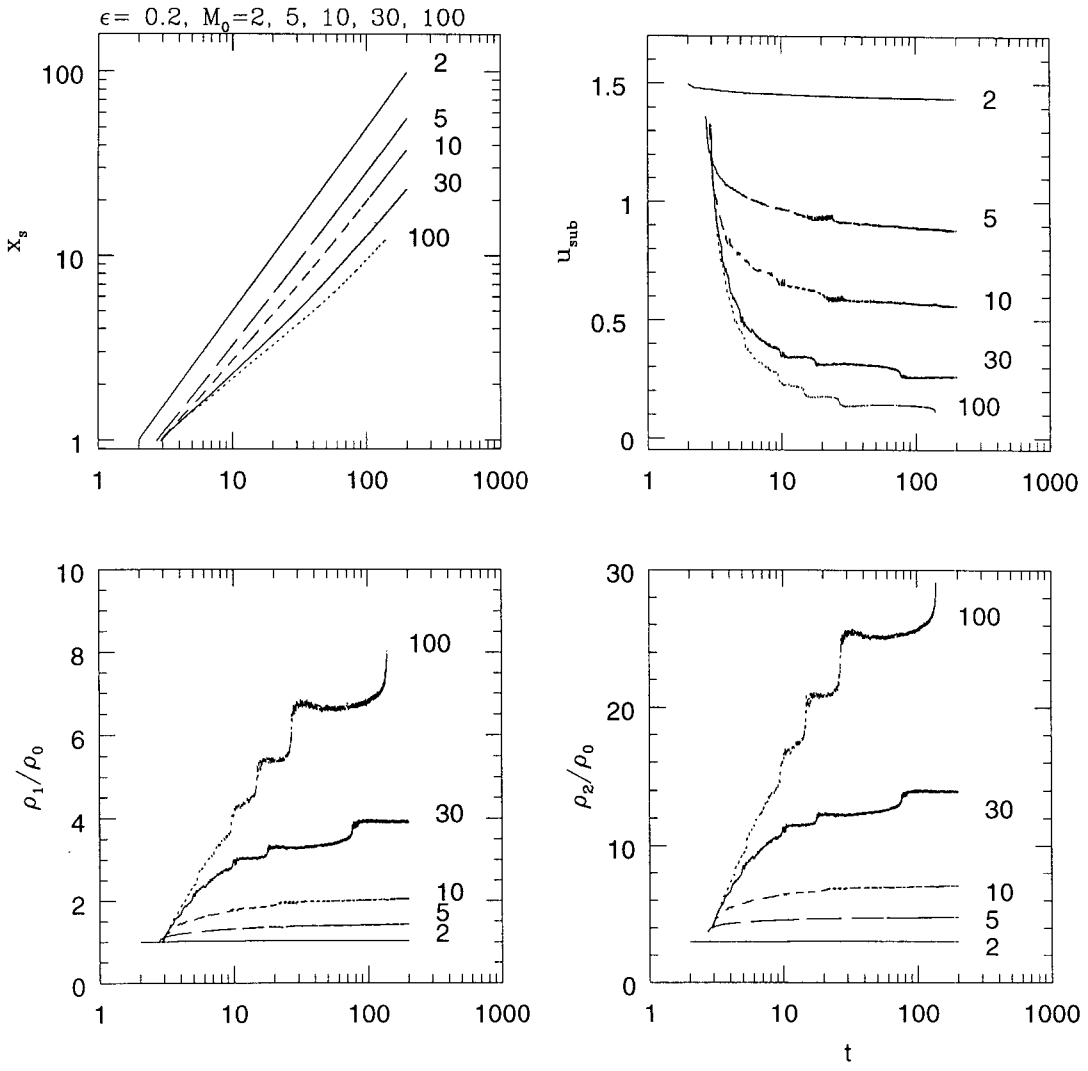

Fig. 7.— Shock location from the reflecting plane, x_s, the shock velocity relative to the immediate preshock flow, $u_{\rm sub}$, preshock density, ρ_1/ρ_0, and postshock density, ρ_2/ρ_0 are plotted as a function of time for $M_0 = 2 - 100$ and $\epsilon = 0.2$.

box from far upstream,

$$\Phi(t) = \frac{\int_0^{x_{max}} {\rm dx} E_{\rm CR}(x,t)}{0.5\rho_0(u'_{s,0})^3 t}. \qquad (16)$$

Since our shock models have the same accretion density and velocity, but different gas pressure depending on M_0, we use the kinetic energy flux rather than the total energy flux to normalize the "CR energy ratio".

In Figure 8 we show the CR energy ratio, Φ, the CR pressure at the shock normalized to the ramp pressure of the upstream flow in the instantaneous shock frame, $P_{\rm c,2}/\rho_0(u'_s)^2$, and the "time-averaged" injection efficiencies, ξ, for shocks with different Mach numbers when $\epsilon = 0.2$ (left three panels). For all Mach numbers the postshock $P_{\rm c,2}$ increases until a balance between injection/acceleration and advection/diffusion of CRs is achieved, and then stays at a steady value afterwards. The time-asymptotic value of the CR pressure becomes, once again, $P_{\rm c,2}/\rho_0(u'_{s,0})^2 \sim 0.56$ and $P_{\rm c,2}/\rho_0(u'_s)^2 \sim 0.8$, for $M_0 = 30$ with $\epsilon = 0.2$. We note that the "undulating" features in the time evolution of $P_{\rm c,2}$ seem to be numerical artifacts and not real. Unlike other spatially averaged or integrated quantities, the plotted $P_{\rm c,2}$ is sampled exactly at the subshock (*i.e.*, from one zone) whose properties show small, noisy variations in time. They seem in particular to correspond to times when the subshock crosses a regular zone boundary and are most prominent for high Mach number models of $M_0 = 30$, and 100. These features can be also seen in the preshock and postshock densities shown in Figure 7.

The CR energy ratio, Φ, increases with time as CRs are injected and accelerated, but it asymptotes to a constant value, once $P_{\rm c,2}$ has reached a quasi-

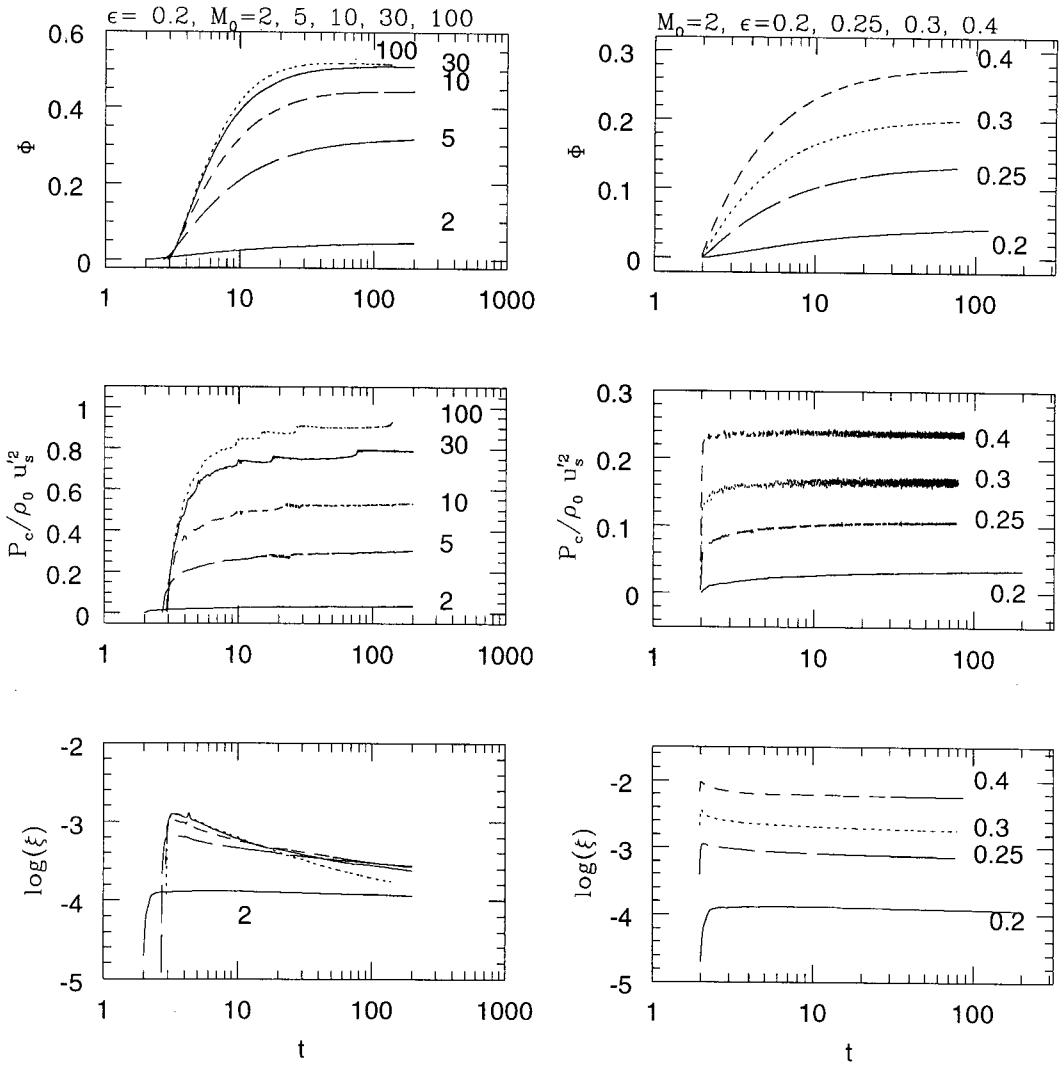

Fig. 8.— The ratio of total CR energy in the simulation box to the kinetic energy in the initial shock rest frame that has entered the simulation box from upstream, $\Phi(t)$, the postshock CR pressure in units of far upstream ram pressure in the instantaneous shock frame, and time-averaged injection efficiency, $\xi(t)$. Left three panels are for $M_0 = 2 - 100$ and $\epsilon = 0.2$. Right three panels show the same quantities for $M_0 = 2$ and $\epsilon = 0.2$, 0.25, 0.3, and 0.4.

steady value. This results from the approximate "self-similar" evolution of the P_c spatial distribution. Time-asymptotic values of Φ increase with M_0 and $\Phi \approx 0.5$ for $M_0 = 30$ at the terminal time.

As discussed in §II(c) in the thermal leakage model the injection rate is higher for higher subshock Mach number, because the ratio of the thermal peak velocity to the injection velocity is smaller. This ratio, however, becomes independent of M_s for $M_{sub} > 10$, so the injection rate also shows the same trend. This Mach number dependence of ξ can be observed in Figure 8, where the initial value of ξ (at $t = 3$) increases with M_0, but it is about the same for $M_0 \geq 10$. After the initial quick increase, it decreases in time as the subshock weakens due to the pre-deceleration in the precursor.

Once again, in order to explore the dependence of our injection model on the parameter ϵ, especially for low Mach shocks, we also show the results for the $M_0 = 2$ ($M_s = 3$) models with $\epsilon = 0.2$, 0.25, 0.3, and 0.4 in the right three panels of Figure 8. As expected, the injection rate is higher for larger values of ϵ, so the CR pressure and Φ are higher. In Kang *et al.* (2002), we made a similar comparison for a wider range of Mach numbers and found that the dependence on ϵ is much weaker for stronger shocks. In a physical model the parameter, ϵ, should depend on the subshock Mach number. But it is not well understood how ϵ should vary with the subshock Mach number for weak shocks. For strong shocks, the average injection rate is about 10^{-3} with $\epsilon = 0.2$, which corresponds to strong wave generation and inefficient leakage. This injection

rate is in fact in a good agreement with what has been observed in the Earth's bow shock (Quest 1988). For $M_s = 3$ shock, the similar injection rate is obtained for $0.25 \leq \epsilon \leq 0.3$, and the CR pressure is about 10-15 % of the shock ram pressure, which could be considered substantial. Then we conclude that CRs can absorb a significant portion of the shock kinetic energy at cosmological shocks, if about $\sim 10^{-3}$ of the particles are injected into the CR component regardless of the details of the injection process.

V. SUMMARY

We have calculated CR acceleration at 1D quasi-parallel shocks by using our CRASH (Cosmic-Ray Amr SHock) code (Kang *et al.* 2002), which incorporates the "thermal leakage" injection process to the CR/hydro code that solves the CR diffusion-convection equation along with CR modified gasdynamic equations. Our simulations are performed in a 1D plane-parallel space in which shocks are generated by the accretion flow reflecting off the central symmetry plane. For convenience, we considered the accretion velocity of $v_{\rm acc} = 1500{\rm kms}^{-1}$ and the magnetic field of 1 microgauss as fiducial values for our simulations. However, the general conclusions can be applied to similar shock speeds, because the CR acceleration is controlled mainly by two physical parameters, the shock Mach number, M_s, and the inverse wave-amplitude parameter, ϵ. The current simulations are similar to those presented in Kang *et al.* (2002), in which freely propagating shocks with open boundaries were considered, except that we adopted a reflecting boundary in the downstream region and our shock velocities, $v_s = 2000 - 2250{\rm kms}^{-1}$, are lower than their value of 3000 $\rm kms^{-1}$. Having the reflecting plane expedites the CR acceleration in our simulations, because CRs are trapped between the shock and the downstream, reflecting, boundary, but otherwise the results are mostly similar. In particular we conclude:

1) Suprathermal particles can be injected very efficiently into the CR population via the thermal leakage process, so that typically a fraction of $10^{-4} - 10^{-3}$ of the particles passed through the shock become CRs for $0.2 \leq \epsilon \leq 0.4$.

2) For a given value of M_s, the injection efficiency is higher for larger values of ϵ (*i.e.,* weaker waves) and so the CR acceleration is more efficient. For example, in the shocks with $M_s = 3$, the ratio $P_{\rm c,2}/\rho_0(u_s')^2$ becomes 0.1, 0.16, and 0.24 for $\epsilon = 0.25$, 0.3, and 0.4, respectively. But this dependency is weaker for higher Mach numbers, so the acceleration efficiency becomes approximately independent of ϵ in the strong shock limits ($M_s \gtrsim 30$).

3) For a given value of ϵ, the acceleration efficiency increases with M_s, but it asymptotes to a limiting value for $M_s \gtrsim 30$. For example, the model with $\epsilon = 0.2$, the ratio of $P_{\rm c,2}/\rho_0(u_s')^2$ becomes 0.03, 0.3, 0.5, 0.8, and 0.9, and the ratio of $P_{\rm c,2}/P_{\rm g,2}$ approaches to 0.05, 0.6, 1.5, 4.9, and 13 for $M_s = 3$, 6.8, 13.3, 40, and 133, respectively.

4) In the strong shock limit of $M \geq 30$, the CR pressure can dominate over the gas pressure and induce a significant precursor where the preshock flow is decelerated adiabatically.

5) The CR pressure seems to approach a time asymptotic value when a balance between acceleration/injection and diffusion/advection processes is achieved, resulting in an approximate "self-similar" flow structure. This is achieved in a time scale comparable to the acceleration time scales for the mildly relativistic protons ($p/m_{\rm p}c \sim 10$), which is much shorter than the cosmological time scale.

We suggest that the CR acceleration at the cosmic shocks are innate to collisionless shock formation process and CRs can absorb a significant fraction of dynamical energy associated with the gravitational collapse during the formation of large scale structure. For strong accretion shocks of $M_s > 10$, CRs can absorb most of shock kinetic energy and the accretion shock speed can be reduced up to 20 %, compared to pure gas dynamic shocks. Although the amount of kinetic energy passed through accretion shocks is small, since they propagate into the low density intergalactic medium, they might possibly provide acceleration sites for ultra-high energy cosmic rays of $E > 10^{18}$eV. For internal merger shocks of $M_s < 3$ the energy transfer to CRs should be less than 10-20 % of the shock kinetic energy at each shock passage, with an associated CR particle fraction of 10^{-3}. Considering that ICM can be shocked repeatedly, however, the CRs generated by merger shocks could be sufficient to explain the observed non-thermal signatures from ICM of galaxy clusters in radio, EUV and X-ray. This implies that the current understandings of cosmological hydrodynamic simulations could be modified by inclusion of this process at a quantitative level of order several tens of percent.

ACKNOWLEDGEMENTS

This work was supported by Korea Research Foundation Grant (KRF-2001-041-D00270). TWJ is supported by NSF grant AST00-71167, by NASA grant NAG5-10774 and by the University of Minnesota Supercomputing Institute.

REFERENCES

Axford, W. I., Leer, E., & McKenzie, J. F. 1982, The structure of cosmic ray shocks, A&Ap, 111, 317

Baring, M. G., Ogilvie, K. W., Ellison, D. C. & Forsyth, R. 1997, Acceleration of Solar Wind Ions by Nearby Interplanetary Shocks: Comparison of Monte Carlo Simulations with ULYSSES Observations ApJ, 476, 889

Bell, A.R. 1978, The acceleration of cosmic rays in shock fronts. I, MNRAS, 182, 147

Berezhko, E., Ksenofontov, L., & Yelshin, V. 1995, Efficiency of CR acceleration in supernova remnants, Nuclear Physic B., 39, 171.

Berezinsky, V. S., Blasi, P. & Ptuskin, V. S. 1997, Clusters of Galaxies as Storage Room for Cosmic Rays, ApJ, 487, 529

Berger, J. S., & LeVeque, R. J. 1998, Adaptive Mesh Refinement using Wave-Propagation Algorithms for Hyperbolic Systems, SIAM J. Numer. Anal., 35, 229 8

Blandford, R. D., & Eichler, D. 1987, Particle Acceleration at Astrophysical Shocks - a Theory of Cosmic-Ray Origin, Phys. Rept., 154, 1

Carilli, C. L., & Taylor, G. B. 2002, Cluster magnetic fields, Annual Rev. Astron. Astrophys., 40, 319

Clark, T.E., Kronberg, P.P., & Böringer, H. 2001, A New Radio-X-Ray Probe of Galaxy Cluster Magnetic Fields, ApJ, 547, L111

Drury, L. O'C. 1983, An Introduction to the Theory of Shock Acceleration of Energetic Particles in Tenuous Plasmas, Rept. Prog. Phys., 46, 973

Ellison, D. C., Möbius, E., & Paschmann, G.1990, Particle injection and acceleration at earth's bow shock - Comparison of upstream and downstream events ApJ, 352, 376

Ensslin, T. A., Lieu, R., & Biermann, P. L., 1999, Non-thermal origin of the EUV and HEX excess emission of the Coma cluster - the nature of the energetic electrons, A&Ap, 344, 409

Feretti, L., Dallacasa, D., Giovannini, G. & Tagliani A., 1995, The magnetic field in the Coma cluster, A&A, 302, 680.

Fusco-Femiano, R., Dal Fiume, D., Feretti, L., Giovannini, G., Grandi, P., Matt, G., Molendi, S., & Santangelo, A. 1999, Hard X-Ray Radiation in the Coma Cluster Spectrum, ApJ, 513, L21

Fusco-Femiano, R., Dal Fiume, D., De Grandi, S., Feretti, L., Giovannini, G., Grandi, P., Malizia, A., Matt, G., & Molendi, S. 2000, Hard X-Ray Emission from the Galaxy Cluster A225, ApJ, 534, L7

Gieseler U.D.J., Jones T.W., & Kang H. 2000, Time dependent cosmic-ray shock acceleration with self-consistent injection, A&Ap, 364, 911

Giovannini, G., Tordi, M., & Feretti, L. 1999, Radio halo and relic candidates from the NRAO VLA Sky Survey, New Astronomy, 4, 141

Jones, T. W., & Kang, H. 1990, Time-dependent evolution of cosmic-ray-mediated shocks in the two-fluid model ApJ, 363, 499

Kang, H., & Jones, T. W. 1991, Numerical studies of diffusive particle acceleration in supernova remnants, MNRAS, 249, 439

Kang, H., Cen, R., Ostriker, J. P., & Ryu D., Hot gas in the cold dark matter scenario: X-ray clusters from a high-resolution numerical simulation, 1994, ApJ, 428, 1.

Kang H., & Jones T.W. 1995, Diffusive Shock Acceleration Simulations: Comparison with Particle Methods and Bow Shock Measurements, ApJ, 447, 944

Kang, H., Ryu, D., & Jones, T. W., 1996, Contributions to the Cosmic Ray Flux above the Ankle: Clusters of Galaxies, ApJ, 456, 422

Kang, H., Rachen, J., & Biermann, P. L. 1997, Contributions to the Cosmic Ray Flux above the Ankle: Clusters of Galaxies, MNRAS, 286, 257

Kang, H., Jones, T. W., LeVeque, R. J., & Shyue, K. M. 2001, Time Evolution of Cosmic-Ray Modified Plane Shocks, ApJ, 550, 737

Kang, H., Jones, T. W., & Gieseler, U.D.J, 2002, Numerical Studies of Cosmic-Ray Injection and Acceleration, ApJ, 579, Nov. 1st issue

Kim, K.-T., Kronberg, P. P., & Tribble, P. C. 1991, Detection of excess rotation measure due to intracluster magnetic fields in clusters of galaxies, ApJ, 355, 29.

Kronberg, P. P., 1994, Rep. Prog. Phys., 325, 382.

Kulsrud, R. M., Cen, R., Ostriker, J. P., & Ryu, D. 1997, The Protogalactic Origin for Cosmic Magnetic Fields, ApJ, 480, 481

LeVeque, R. J., & Shyue, K. M. 1995, One-dimensional front-tracking based on high resolution wave propagation methods, SIAM J. Scien. Comput. 16, 348

Lieu, R., Ip, W.-H., Axford, W. I., & Bonamente, M. 1999, Nonthermal Origin of the EUV and Soft X-Rays from the Coma Cluster: Cosmic Rays in Equipartition with the Thermal Medium, ApJ, 510, L25

Loeb, A & Waxmann, E., 2000, Cosmic .-ray background from structure formation in the intergalactic medium, Nature, 405, 156

Lucek, S.G., & Bell, A.R. 2000, Non-linear amplification of a magnetic field driven by cosmic ray streaming, MNRAS, 314, 65

Malkov, M.A. 1998, Ion leakage from quasiparallel collisionless shocks: Implications for injection and shock dissipation, Phys. Rev. E, 58, 4911,

Malkov, M.A., & Völk H.J. 1998, Diffusive ion acceleration at shocks: the problem of injection, Adv. Space Res. 21, 551

Malkov M.A., & Drury, L.O'C. 2001, Nonlinear theory of diffusive acceleration of particles by shock waves, Rep. Progr. Phys. 64, 429

Miniati, F., 2002 Inter-galactic Shock Acceleration and the Cosmic Gamma-ray Background, astro-ph/0203014

Miniati, F., Ryu, D., Kang, H., Jones, T. W., Cen, R., & Ostriker, J. 2000, Properties of Cosmic Shock Waves in Large-Scale Structure Formation, ApJ, 542, 608

Miniati, F., Ryu, D., Kang, H., & Jones, T.W. 2001a, Cosmic-Ray Protons Accelerated at Cosmological Shocks and Their Impact on Groups and Clusters of Galaxies, ApJ, 559, 59

Miniati, F., Jones, T. W., Kang, H., & Ryu, D. 2001b, Cosmic-Ray Electrons in Groups and Clusters of Galaxies: Primary and Secondary Populations from a Numerical Cosmological Simulation, ApJ, 562, 233

Norman C. A., Melrose D. B., & Achterberg A., The Origin of Cosmic Rays above 10 18.5 eV, 1995, ApJ, 454, 60

Quest, K.B. 1988, Theory and simulation of collisionless parallel shocks, J. Geophys. Res. 93, 9649

Ryu, D., Kang, H., & Biermann, P. L. 1998, Cosmic magnetic fields in large scale filaments and sheets, A&AP, 335, 19

Sarazin, C. L. 1999, The Energy Spectrum of Primary Cosmic-Ray Electrons in Clusters of Galaxies and Inverse Compton Emission, ApJ, 520, 529

Sarazin, C. L., & Lieu, R., 1998, Extreme-Ultraviolet Emission from Clusters of Galaxies: Inverse Compton Radiation from a Relic Population of Cosmic Ray Electrons?, ApJ, 494, L177

Scharf, C. A. & Mukherjee, R., 2002 A statistical detection of gamma-ray emission from galaxy clusters: implications for the gamma-ray background and structure formation, astro-ph/0207411

Skilling, J. 1975, Cosmic ray streaming. I - Effect of Alfvén waves on particles, MNRAS, 172, 557

Taylor, G. B., Barton, E. J., & Ge, J. P., 1994, Searching for cluster magnetic fields in the cooling flows of 0745-191, A2029, and A4059, AJ, 107, 1942.